Selective Sensitivity of Open Chaotic Flows on Inertial Tracer Advection: Catching Particles with a Stick

I. J. Benczik,[1] Z. Toroczkai,[2] and T. Tél[1]

[1]*Institute for Theoretical Physics, Eötvös University, P.O. Box 32, H-1518 Budapest, Hungary*

[2]*Complex Systems Group, Theoretical Division, Los Alamos National Laboratory, Los Alamos, New Mexico 87545*

(Received 30 April 2002; published 25 September 2002)

We investigate the effects of finite size and inertia of a small spherical particle immersed in an open unsteady flow which, for ideal tracers, generates transiently chaotic trajectories. The inertia effects may strongly modify the chaotic motion to the point that attractors may appear in the configuration space. These studies are performed in a model of the two-dimensional flow past a cylindrical obstacle. The relevance to modeling efforts of biological pathogen transport in large-scale flows is discussed. Since the tracer dynamics is sensitive to the particle inertia and size, simple geometric setups in such flows could be used as a particle mixture segregator separating and trapping particles.

DOI: 10.1103/PhysRevLett.89.164501 PACS numbers: 47.52.+j, 05.45.Jn, 07.07.Df, 47.55.Kf

It has been shown both theoretically [1–3] and experimentally [4,5] that the presence of a particle with nonzero mass and size modifies the flow locally and, therefore, the motion of such a particle in the fluid typically differs from that of an ideal tracer, which simply follows the local velocity of the flow.

The breath of practical applicability of such studies is large, ranging from atmospheric sciences (such as pollutant transport, cloud formation, balloons) to chemical engineering and industrial applications (see, for example, the excellent reviews by Michaelides [3] on the equations of motion, Sirignano [6] on spray dynamics, and Stock [7] on turbulence and dispersion in gases). One important, and probably less known, application of these studies is aerosol and pollutant transport forecasting for homeland defense and threat reduction purposes supporting short term decision response in case of a toxin or biological pathogen spill in large-scale flows. Current models consider the particle transport as if it were passive, but this limitation can be rather severe, causing errors of order one in computing tracer trajectories, as we show below.

For spherical tracer particles of radius a the tracer velocity $\mathbf{v}$ typically differs from the fluid velocity $\mathbf{u}$. The equation of motion is given by Newton's law: The force causing a relative acceleration $d\mathbf{v}/dt - d\mathbf{u}/dt$ between tracer and fluid is due to the viscous friction. We shall assume in what follows that buoyancy effects are negligible. The Stokes drag is proportional to the velocity difference $\mathbf{v} - \mathbf{u}$, and vanishes for pointlike tracers. In dimensionless form the equation of motion reads [1,8]

$$\frac{d\mathbf{v}}{dt} - \frac{3}{2}R\frac{d\mathbf{u}}{dt} = -A(\mathbf{v} - \mathbf{u}) \tag{1}$$

where the parameters are the "mass ratio" R,

$$R = \frac{2\rho_f}{\rho_f + 2\rho_p}, \tag{2}$$

and the "inertia parameter" A given by

$$A = R/St, \qquad \mathrm{St} = \frac{2}{9}\left(\frac{a}{L}\right)^2 \mathrm{Re}, \tag{3}$$

where ρ_f and ρ_p are the densities of the fluid and of the particle, St is the Stokes number (or the dimensionless decay time due to the Stokes drag), $\mathrm{Re} = UL/\nu$ is the fluid Reynolds number, L is a typical large-scale length, and U is a typical large-scale fluid velocity. The presence of the coefficient $3R/2$ expresses the fact that an inertial particle brings into motion a certain amount of fluid, proportional to half of its volume. This added mass effect is not present for neutrally buoyant particles for which $R = 2/3$. In terms of the mass ratio parameter, if $R < 2/3$, the particle is heavier than the fluid, also called *aerosol* [9], and in the range $2/3 < R < 2$ it is lighter than the surrounding fluid and is called *bubble* [9]. The tracer Eq. (1) is derived for initial tracer velocities matching the fluid velocity. The limit $A \to \infty$ corresponds to the passive ideal tracer limit. The smaller A, the more pronounced is the effect of inertia. This effect can be of order one even for very small particles in a flow with chaotic Lagrangian dynamics [10,11], or turbulent flows [8]. A simple estimate [12] shows that this effect can become significant for anthrax spores. For nonturbulent, low Reynolds number flows, with Re on the order of hundreds, the particle dynamics is typically *chaotic* [13–15]. This means that small deviations in particle trajectories grow exponentially in time at a rate given by the largest positive Lyapunov exponent of the dynamics which is influenced by the inertia parameters. The general inertial dynamics (1) possesses a five-dimensional phase space for two-dimensional flows. The inertial motion is dissipative. In incompressible flows, to which we restrict ourselves, the phase-space contraction rate is easily computed from (1) to be $2A$, i.e., *positive*. This opens the possibility of having attractors in the dynamics. Note that such attractors or any other invariant sets exist in the *full* phase space, but what we observe is always a

projection of these sets onto the configuration space (the plane of the flow).

In this Letter we study inertia effects in the wake of obstacles (such as a stick, a pillar, or an island) for two-dimensional flows, where the Eulerian velocity is smooth in space and periodic in time. Ideal tracers are known to exhibit in such open time periodic flows transient chaos [16]: they can stay in the wake over finite times, but ultimately *all* the particles escape. This behavior is in contrast to the everyday observation according to which light objects, like, e.g., empty Coke cans, can be trapped in the wake for arbitrarily long times. This can be explained with Eq. (1), since it is strongly dissipative. It is surprising, however, that the attractor is not the obstacle's surface (covered by a "sticky" boundary layer), but a set of *periodic or chaotic orbits* in the wake. As we show below, this may hold only for light tracers (bubbles, $R > 2/3$).

For concreteness we consider a model of the von Kármán vortex street in the wake of a cylinder [16]. Because of the incompressibility of the flow, a stream function $\mathbf{\Psi} = [0, 0, \Psi(x, y, t)]$ can be defined such that the fluid velocity will be given by the Hamiltonian form $\mathbf{u} = \nabla \times \mathbf{\Psi}$. In Ref. [16] an explicit expression for Ψ was given, approximating the Navier-Stokes equations with $\mathrm{Re} \simeq 250$. One of the parameters entering the model's stream function is the average strength of the detaching vortices, w, which we are fixing here to be $w = 24 \times 8/\pi$; see [17] for details. The length is measured in units of the cylinder radius, which is simultaneously the characteristic linear size L of the flow, and the period T of the flow is taken as the time unit. Figure 1 shows a comparison between trajectories started with the same initial conditions but different inertia parameters A and mass ratio R.

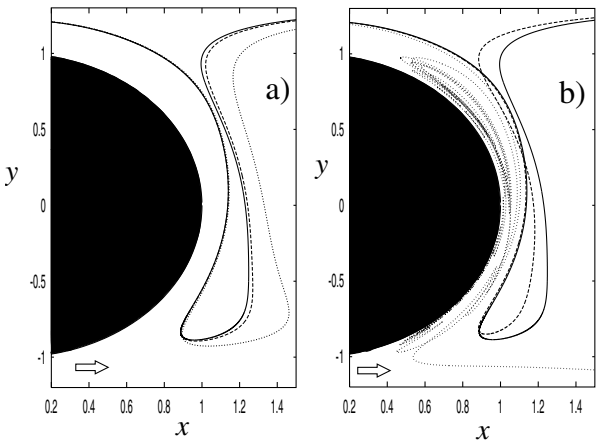

FIG. 1. Inertial and passive tracer trajectory comparison. (a) Aerosol regime $R = 0.6$; $A = 1000$, dashed line; $A = 150$, dotted line. (b) Bubble regime $R = 1.4$; $A = 2000$, dashed line; $A = 200$, dotted line. All trajectories were started from $x = -2.0$, $y = 0.0758$ at time $t_0 = 0.3$. The continous line is the passive tracer's trajectory. The arrows point in the downstream direction.

For aerosols, the particles exit the wake faster on average, since the centrifugal force along any closed orbit is pushing the heavier particle outward. Bubbles can be trapped longer by the vortices in the wake; see Fig. 1(b). A statistical measure of the sensitive selectivity of the flow on the inertia and mass parameters is obtained from the study of the escape rate κ [18] for an ensemble of particles initially covering the wake. We observe an exponential escape regime of the particles caused by the existence in the wake of a chaotic hyperbolic saddle. As seen from Fig. 2, the decay rates are dependent on the parameters A and R.

In the following we concentrate on the bubble regime ($R > 2/3$) only. Our main observation is that in contrast with the passive case, bubbles *can get trapped permanently* in the wake of the obstacle. This means that the inertia can modify the dynamics to the point where attractors appear in the phase space with a visible component in the configuration space. In order to show this, in Fig. 3 we present the residence time of the tracer on the plane of initial conditions. The shades of blue, yellow, and red depict residence times in increasing order. Dark red corresponds to initial conditions that lead to permanently trapped particles. The cylinder is shaded dark blue. Thus, the dark red domains correspond to the *basin of attraction* of the attractors that appeared in the configuration space. These basins of attraction are of finite area and extend upstream. A second important observation is that the longer lifetime of chaos, and trapping, is not only due to the surface of the cylinder. The attractors are actually situated in the wake, *away* from the boundary of the cylinder. Because of the symmetry [19] of the flow we have two copies of the attractor, one above the symmetry axis ($y = 0$) and the other below. The attractors on Fig. 3 are period-two cycles. At smaller values of R they become chaotic (Fig. 4). As R increases, these chaotic

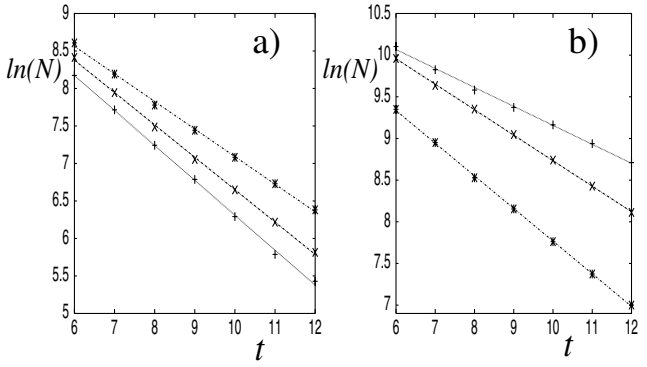

FIG. 2. The escape rate κ is the slope of the $\ln N$ vs t plot. We started an $N(0) = 1000 \times 1000$ particle droplet from the domain $[0, 2.0] \times [-1, 1]$ around the cylinder and measured the number $N(t)$ of particles remaining there up to time t. (a) Aerosol regime $R = 0.6$ for $A = 30(+), 90(X), 200(*)$, $\kappa = 0.46, 0.43, 0.36$. (b) Bubble regime $R = 4/3$ for $A = 60(+), 90(\times), 200(*)$, $\kappa = 0.23, 0.31, 0.39$.

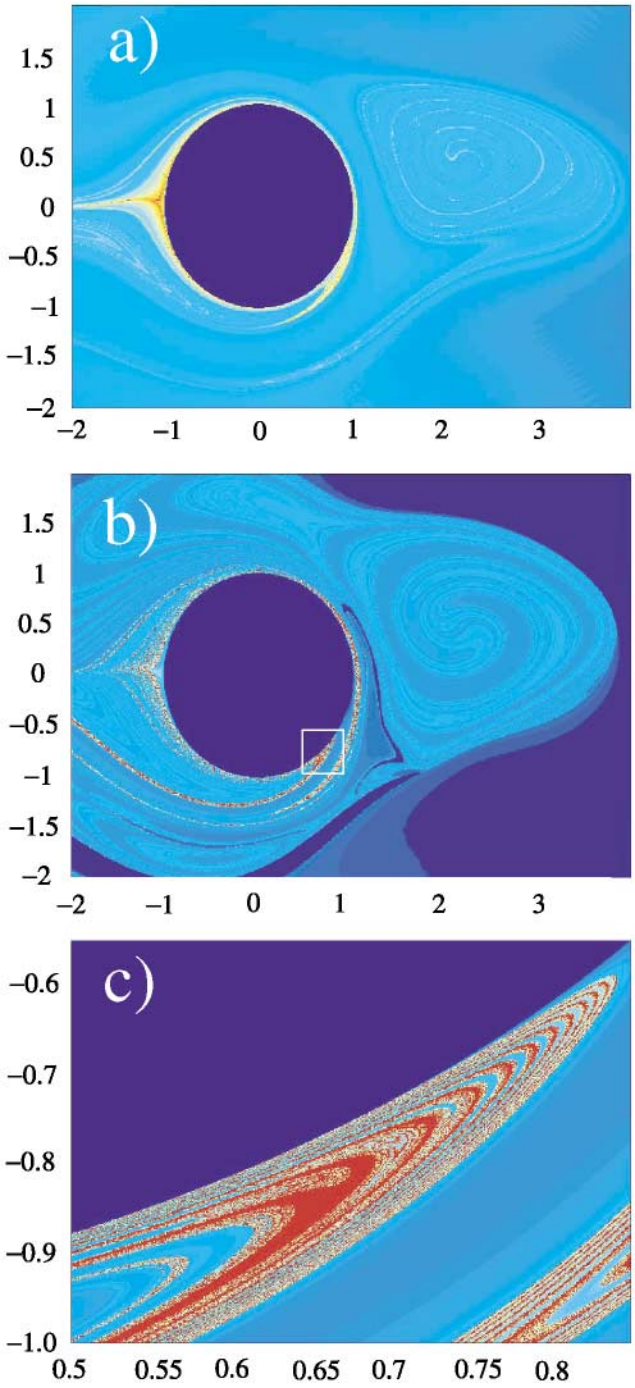

FIG. 3 (color). Residence times for an ideal passive tracer (a) and for a bubble tracer (b) and (c). We started a particle from every point (x, y) of a grid (540×540) covering the region around the cylinder, and measured the time it took for the particle to leave this region. Here $A = 30$, $R = 1.55$. (c) The magnification of a small rectangle from (b).

attractors are transformed in two isolated periodic orbits through an *inverse period-doubling sequence* [Fig. 4(c)].

For example, at $R = 1.7$ $(A = 30)$ the attractor (on either side of $y = 0$) is a period $T = 1$, bean-shaped loop. A bounded particle trajectory can exist only if the particle velocity is for some time faster, for some time slower than the flow; see Fig. 5.

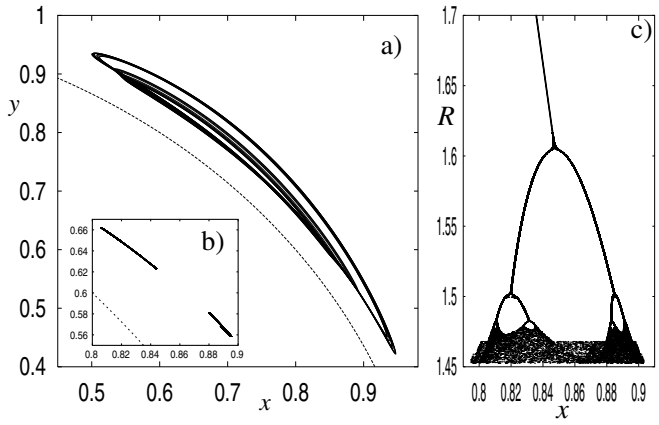

FIG. 4. The chaotic attractor in the upper half plane at $R = 1.47, A = 30$. (a) A continuous time plot of the attractor, whereas the inset, (b), shows the same attractor on the stroboscopic map (which is a tight filamental structure not resolved in the inset). The dashed lines represent the cylinder's surface. (c) This chaotic attractor goes into a fixed point (on the stroboscopic map) as R is increased.

The phenomenon of trapping is a *generic* property resulting from the nonlinear interaction of the *temporal dependence* of the underlying flow and inertia parameters.

In order to show this we now present a proof-of-principle type of calculation in the case of a simple, generic flow model, which exhibits a single hyperbolic fixed point in the origin (so a passive tracer would be repelled to infinity), and show that there is a parameter regime for *bubbles* where this fixed point becomes *attracting* and thus the motion bounded.

Let us consider the pulsating isochoric stream function: $\Psi(x, y, t) = G(t)(\frac{1}{2}y^2 - \frac{K}{2}x^2)$, with $G(t) = 1 + L\sin\omega t$, and $L, K \in \mathbb{R}$, $\omega > 0$. For $L = 0$ we obtain the classic isochoric stream function which for $K < 0$ produces elliptic motion, for $K = 0$ a shear flow, and for $K > 0$ hyperbolic motion for a passive ideal tracer ([14], p.29).

One can analytically check that for any inertial parameters the origin remains hyperbolic for $K > 0$, as long as the stream function is *time independent* $(L = 0)$. On the other hand, if the stream function is time dependent $(L \neq 0)$, the hyperbolic origin can become attractive for bubbles. Notice that the time dependence we introduced in Ψ is simply a multiplicative factor. Thus, the passive tracer trajectories will *coincide* with those for the time-independent stream function, and for $K > 0$ the passive tracer motion is unbounded (with a temporally oscillating component *along* these hyperbolic trajectories). Let $\mathbf{z} = (x, y, v_x, v_y)$ be the phase-space vector for the inertial particle. From (1) we obtain the equations of motion as $\dot{\mathbf{z}} = \mathbf{M}(t)\mathbf{z}$, where the nonzero entries of the time-dependent matrix are $M_{13} = 1$, $M_{24} = 1$, $M_{31} = \alpha G^2 K$, $M_{32} = AG + \alpha\dot{G}$, $M_{33} = -A$, $M_{41} = M_{32}K$,

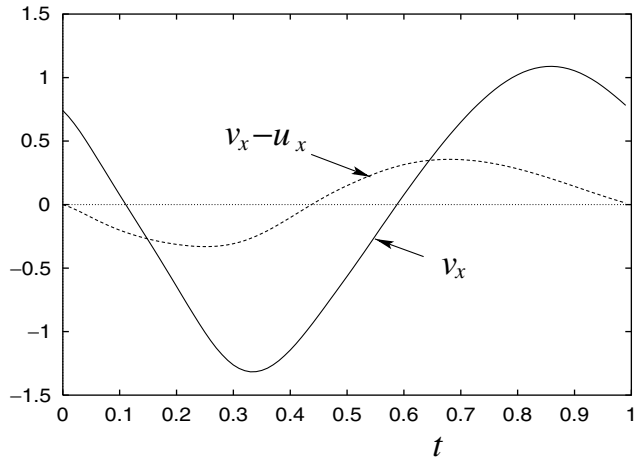

FIG. 5. The velocity component v_x of the bubble and relative velocity $v_x - u_x$ between the particle and the flow along a period-1 attractor ($A = 30$, $R = 1.7$). The integral of $v_x - u_x$ is zero over one period.

$M_{42} = M_{31}$, $M_{44} = M_{33}$, with the shorthand $\alpha = 3R/2$, $\dot{G} = dG/dt$. Unfortunately, this system cannot be solved analytically. Numerically, it is very easy to find parameter values where the origin becomes attractive for $K > 0$. For example, $\{K = 1.0, A = 30, R = 1.8, \omega = 10\pi, 5.99 \leq L \leq 13.63\}$, or $\{K = 0.2, A = 20, R = 1.3, \omega = 6\pi, L = 15.0\}$, etc. In the following we present a *necessary* condition for the stability of $\mathbf{z} = 0$. To do this, for simplicity we first set $K = 1$. If we introduce the variables $Z(t) = x(t) + y(t)$, $V(t) = v_x(t) + v_y(t)$, the equations of motion reduce to $\dot{Z} = V$, and $\dot{V} = -AV + a(t)Z$, or $\ddot{Z} + A\dot{Z} = a(t)Z$, where $a(t) = \alpha G(t)^2 + AG(t) + \alpha\dot{G}(t)$, a periodic function of time. The initial conditions must satisfy $V(t_0) = G(t_0)Z(t_0)$. The $Z(t)$ variable describes the projection of the motion to the first bisector. Bounded motion in the (x, y) coordinates implies boundedness in Z as well. With the transformation $U = \dot{Z}/Z + A/2$, the equation becomes

$$\dot{U} + U^2 = b(t), \tag{4}$$

with $b(t) = A^2/4 + a(t)$. Note that this type of nonlinearity is inherent in [1]. The same type of equation is obtained for the gradient of the velocity of rain droplets taken at the droplet's trajectory [20] using (1). If the solution to (4) is known, the solution in Z is obtained via $Z(t) = Z_0 \exp[-A(t - t_0)/2 + \int_{t_0}^{t} U(s)]$. This means that if $\overline{U} = \lim_{t\to\infty}(1/t)\int_0^t U(s) > A/2$, the origin is attracting: for $\overline{U} = A/2$ it is marginally stable, and for $\overline{U} < A/2$ it is repelling or unstable.

We have shown the possibility that by a proper engineering of the geometry of the open *chaotic* flow, selective inertial particle traps can be designed. The trapping phenomenon is at the same time a warning that a simple modeling of inertial particles as passive ideal tracers can lead to gross errors in forecasting particle motion. Our example shows that a harmful substance while modeled as a passive tracer will clear the wake of an obstacle , but in reality it may be indefinitely trapped there under the same conditions.

We are grateful for useful conversations with M. Chertkov, R. E. Ecke, G. Falkovich, M. Hastings, L. Margolin, and O.Piro. Z. T. was supported by the DOE, Contract No. W-7405-ENG-36. The support of the Hungarian Science Foundation (OTKA, No. TO32423) and the MTA-OTKA-NSF Grant No. 526 are acknowledged.

[1] M. R. Maxey and J. J. Riley, Phys. Fluids **26**, 883 (1983).
[2] T. R. Auton *et al.*, J. Fluid Mech. **197**, 241 (1988).
[3] E. E. Michaelides, J. Fluids Eng. **119**, 233 (1997).
[4] G. Segre and A. Silberberg, Nature (London) **189**, 209 (1961); J. Fluid Mech. **14**, 115 (1962).
[5] T. Shinbrot *et al.*, Phys. Rev. Lett. **86**, 1207 (2001).
[6] W. A. Sirignano, J. Fluids Eng. **115**, 345 (1993).
[7] D. E. Stock, J. Fluids Eng. **118**, 4 (1996).
[8] E. Balkovsky, G. Falkovich, and A. Fouxon, Phys. Rev. Lett. **86**, 2790 (2001).
[9] M. R. Maxey, Phys. Fluids **30**, 1915 (1987).
[10] A. Babiano *et al.*, Phys. Rev. Lett. **84**, 5764 (2000).
[11] T. Nishikawa, Z. Toroczkai, and C. Grebogi, Phys. Rev. Lett. **87**, 038301 (2001); T. Nishikawa, Z. Toroczkai, C. Grebogi, and T. Tél, Phys. Rev. E **65**, 026216 (2002).
[12] For example, anthrax spores being of organic nature, their density is somewhat less than but comparable to that of the water ($0.1 < \rho_p < 1$), and $a \simeq 1$–20 μm. Anthrax in air has a mass ratio $10^2 < \rho_{\text{ant}}/\rho_{\text{air}} < 10^3$ and classifies as a "heavy" particle. In water, however, this ratio is $0.1 < \rho_{\text{ant}}/\rho_{\text{wat}} < 1.0$ and classifies as "light." In air, for example, $A \simeq (10^7$–$10^{12})/\text{Re}$ which can obviously lead to significant effects for turbulent flows.
[13] H. Aref, J. Fluid Mech. **143**, 1 (1984).
[14] J. M. Ottino, *The Kinematics of Mixing: Stretching, Chaos and Transport* (Cambridge University Press, Cambridge, 1989).
[15] S. Wiggins, *Chaotic Transport in Dynamical Systems* (Springer, New York, 1992).
[16] C. Jung, T. Tél, and E. Ziemniak, Chaos **3**, 555 (1993).
[17] I. J. Benczik *et al.* (to be published).
[18] T. Tél, in *Directions in Chaos*, edited by Hao Bai-Lin (World Scientific, Singapore, 1990), Vol. 3, p. 149.
[19] The symmetry is $(x, y, t) \leftrightarrow (x, -y, t \pm T/2)$.
[20] G. Falkovich, A. Fouxon, and M. G. Stepanov (to be published); M. R. Maxey, J. Fluid Mech. **226**, 1 (1987).